KSÜ Tarım ve Doğa Derg 26 (5), 977-990, 2023
KSU J. Agric Nat 26 (5), 977-990, 2023
https://doi.org/10.18016/ksutarimdoga.vi.1120643

Green Synthesis, Characterization, and Evaluation of Biocompatible Structures of Gold Nanoparticles in Biomedical Applications (Antibacterial, Antifungal, and Anticancer)

Ayşe BARAN[1], Cumali KESKIN[2]✉
[1]Department of Biology, Graduate Education Institute, Mardin Artuklu University, Mardin, Türkiye, [2]Department of Medical Services and Techniques, Vocational Higher School of Healthcare Studies, Mardin Artuklu University, Mardin, Türkiye
[1]https://orcid.org/0000-0002-2317-0489,[2]https://orcid.org/0000-0003-3758-0654
✉: cumalikeskin@artuklu.edu.tr

ABSTRACT
Gold nanoparticles (AuNPs) stand out due to their low toxicity and high compatibility, and the large and modifiable surface areas they provide. In this study, the leaves of *Celtis tournefortii* Lam. (CT) were used for the green synthesis of gold nanoparticles (AuNPs) first time. The size, shape, surface charge, and functionality of the synthesized AuNPs are described in detail. The suggested mechanisms of action on the tested target cells are highlighted. The biological activities (antibacterial, antifungal, and anticancer) of "green" AuNPs and their further biomedical application possibilities are also discussed. Synthesized AuNPs displayed a spherical appearance, surface plasmon resonance band at 553.67 nm wavelength, and surface charge of -16.53 mV. Particle morphology, size, and surface charge were observed to be affected by the leaf extract used in the reduction reaction. FTIR and TGA-DTA data revealed that functional groups from the CT extract participate in the synthesis and stabilization of AuNPs. AuNPs showed antibacterial and antifungal effects on all the strains and yeast tested by microdilution method (MIC). AuNPs showed dose-dependent cytotoxic activity on cancerous cell lines (SKOV-3, CaCo2, and U118). The obtained results highlight a potentially low-cost green synthesis method using CT leaf extract to synthesize AuNPs showing important biological properties.

Biochemistry

Research Article

Article History
Received : 24.05.2022
Accepted : 14.02.2023

Keywords
AuNPs
Antipathogenic
Celtis tuernofortii Lam
Green Synthesis
Nanomedicine

Altın Nanopartiküllerin Yeşil Sentezi, Karakterizasyonu ve Biyouyumlu Yapılarının Biyomedikal Uygulamalarda (Antibakteriyel, Antifungal ve Antikanser) Değerlendirilmesi

ÖZET
Altın nanopartiküller (AuNP'ler), toksisitelerinin düşük olması ve yüksek uyumlulukları ile sağladıkları geniş ve düzenlenebilen yüzey alanlarının olmasından dolayı dikkat çekmektedirler. Bu çalışmada, *Celtis tuernofortii* Lam. (CT) yaprakları altın nanoparçacıkların (AuNP'ler) yeşil sentezi için ilk kez kullanıldı. Sentezlenen AuNP'lerin boyutu, şekli, yüzey yükü ve işlevselliği ayrıntılı olarak tanımlandı. Test edilen hedef hücreler üzerinde önerilen etki mekanizmaları vurgulandı. "Yeşil" AuNP'lerin biyolojik aktiviteleri (antibakteriyel, antifungal ve antikanser) ve bunların diğer biyomedikal uygulama olasılıkları da tartışıldı. Sentezlenen AuNP'ler küresel bir görünüm, 553.67 nm dalga boyunda yüzey plazmon rezonans bandı ve -16.53 mV yüzey yükü sergiledi. Partiküllerin morfolojisi, boyutu ve yüzey yükünün indirgeme reaksiyonunda kullanılan yaprak ekstraktından etkilendiği gözlemlendi. FTIR ve TGA-DTA verileri, CT özünden elde edilen fonksiyonel grupların AuNP'lerin sentezine ve stabilizasyonuna katıldığını ortaya koydu. AuNP'ler, mikrodilüsyon yöntemi (MIC) ile test edilen tüm suşlar ve mayalar üzerinde antibakteriyel ve antifungal etkiler gösterdi. AuNP'ler kanser hücre hatları (SKOV-3, CaCo2 ve U118) üzerinde doza bağlı sitotoksik aktivite gösterdi. Elde edilen sonuçlar, önemli biyolojik özellikler gösteren AuNP'leri sentezlemek için CT yaprak özütü kullanan, potansiyel olarak düşük maliyetli bir yeşil sentez yöntemini vurgulamaktadır.

Biyokimya

Araştırma Makalesi

Makale Tarihçesi
Geliş Tarihi : 24.05.2022
Kabul tarihi : 14.02.2023

Anahtar Kelimeler
AuNP'ler
Antipatojenik
Celtis tuernofortii Lam.
Yeşil sentez
Nanotıp

Atıf Şekli: Baran, A., & Keskin, C., (2023) Altın Nanopartiküllerin Yeşil Sentezi, Karakterizasyonu ve Biyouyumlu Yapılarının Biyomedikal Uygulamalarda (Antibakteriyel, Antifungal ve Antikanser) Değerlendirilmesi. *KSÜ Tarım ve Doğa Derg 26* (5), 977-990. https://doi.org/10.18016/ksutarimdoga.vi.1120643

To Cite : Baran, A., & Keskin, C., (2023). Green Synthesis, Characterization, and Evaluation of Biocompatible Structures of Gold Nanoparticles in Biomedical Applications (Antibacterial, Antifungal, and Anticancer). *KSU J. Agric Nat 26*(5), 977-990. https://doi.org/10.18016/ksutarimdoga.vi.1120643

INTRODUCTION

Nanotechnology is growing rapidly for the production of new materials in this field, and these products at the nanoscale level have superior features such as large superficial area, magnetic, optical, and conductibility (Velmurugan et al., 2014; Baran 2019a). Among these products, studies with metallic nanoparticles (MNPs) such as gold (Au), silver (Ag), titanium (Ti), iron (Fe), copper (Cu), and zinc (Zn) are the most favored (Asghar et al., 2018; Baran, et al., 2019; Baran, 2019; Pandiyan et al., 2019; Baran, et al., 2021). There are various approaches such as biological, physical, and chemical protocols to produce nanoparticles. Among the biological synthesis protocols, plant-based synthesis processes attract a lot of attention thanks to their advantages such as ease, not requiring special conditions, and excess product (Al-ogaidi et al. 2017, Patil et al. 2018, Rolim et al. 2019). The leaves (Baran, 2019b), roots (Marslin et al. 2015), flowers (Remya et al. 2015), and sometimes the whole plant can be used in the synthesis of NPs. Functional groups of phytochemicals found in plant sources (such as phenolic groups, alcohol groups, and amine groups) are considered responsible for the formation of metallic nanoparticles, the biological reduction of metals, and also in stabilization (Shankar et al. 2016; Some et al. 2019).

Recent studies agree on the diverse advantages of nanogold upon dissimilar nanomaterials, primarily owing to immensely optimized methods for the generation of gold nanoparticles of numerous dimensions and shapes, featuring together exclusive characteristics. The AuNPs are among the important NPs used in diagnosis and treatment in biomedical applications (Rautray and Rajananthini 2020). AuNPs are accepted as medical agents for anticancer, antimicrobial, anti-inflammatory, and antidiabetic applications. Moreover, they are used as theragnostic implementation for various diseases such as cancer, diabetes, Parkinson's, Alzheimer's, AIDS, arthritis, hepatitis, cirrhosis, spinal cord injury, tuberculosis, and circulatory system diseases (Patra et al. 2015, Kumar et al. 2017, Mohammadi et al. 2019, Abu-Dief et al. 2020, Arroyo et al. 2020).

Antibiotic resistance is a serious problem. In the face of resistance developed by microorganisms, the search for antimicrobial agents maintains its importance. Many studies are explaining that AuNPs synthesized by bioderived synthesis methods show effective antimicrobial activity (Donga et al. 2020, Tripathy et al. 2020, Hatipoğlu 2021, Mandhata et al. 2021, Mehravani et al. 2021).

Cancer, which is a difficult disease to treat that many people around the world are trying to fight, constitutes an important field of study where various methods are researched for its treatment, and alternative methods are developed day by day. Effective and positive results have been obtained in studies that foresee the use of AuNPs, which are synthesized by environmentally friendly synthesis methods, as an anticancer agent due to their biocompatible properties (González-Ballesteros et al. 2017, Haddada et al. 2019, Satpathy et al. 2020, Padalia & Chanda 2021).

Celtis tournefortii Lam., which is called by various names such as "Dağdagan", is a member of the *Ulmaceae* family and is a deciduous tree that grows in tropical regions and high temperate regions, with an average height of five meters. It grows in countries such as Turkey, Azerbaijan, Iran, Iraq, Greece, Croatia, and Ukraine. In studies conducted to determine the chemical contents of the genus *Celtis*, it has been stated that it contains phytochemicals such as phenolic acids, coumarins (coumarin, esculetine), tannins (gallic acid, flavan-3-ols (catechins), chlorogenic acid), flavonoids (quercetin, rutin, naringenin), steroids (brassinosteroids), terpenoids (menthol, geraniol), and alkaloids (caffeine, capsaicin) (Keser et al., 2017; Yıldırım et al., 2017; Holopainen et al., 2018; Gecibesler, 2019; Baran et al., 2022).

Therefore, the present study focused to improve the green synthesis and characterization of AuNPs using the aqueous extract from fresh *C. tournefortii* plant leaves and to study the antimicrobial, antifungal, and anticancer activities.

MATERIALS and METHODS

Materials

Leaves were collected from *C. tournefortii* L. trees (oriental hackberry, dağdağan) at the end of August in Mardin Kızıltepe Region (at position 37°17' 07.3" N and 40° 29' 03.0" E) (Figure 1). After pre-washing with tap water, washing was also done with distilled water. It was dried at room condition and prepared for extraction. Then, 100 g of the dried leaves were weighed and mixed with 500 ml of distilled water and allowed to boil on the heater. It was cooled at room conditions, filtered with filter paper, taken at +4 °C, and made ready for synthesis. A solution with a concentration of five millimolar (mM) was prepared from the compound Alpha Aesar Tetrachloroauric (III) acid trihydrate (in Kandel, Germany).

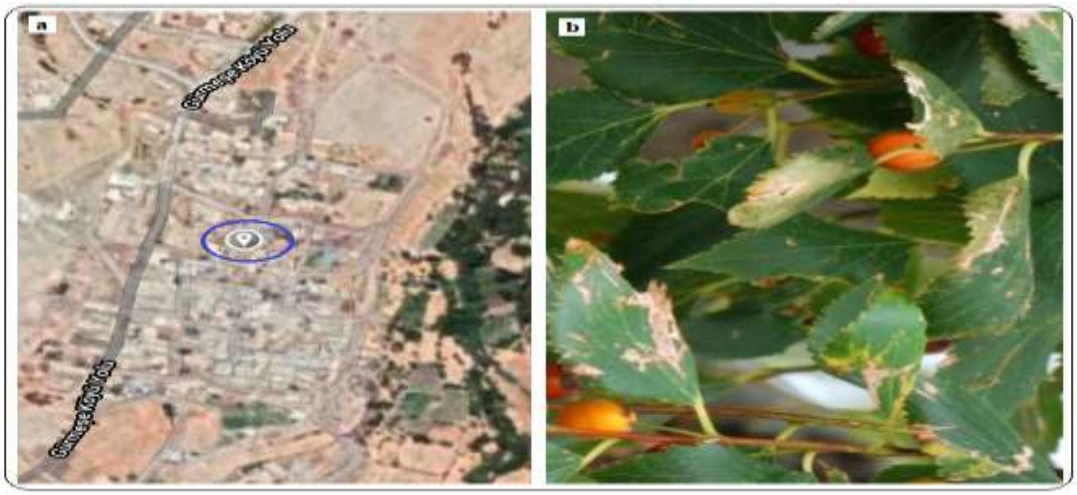

Figure 1. Plant of *C. tournefortii* L. a. location information, b. morphological view of leaves
Şekil 1. Celtis tournefortii Lam. Bitkisinin; a. yetiştiği alana ait konum, b. bitki yapraklarının morfolojik görünümü

Synthesis and Characterization of CT-AuNPs

The extract prepared using C. tournefortii (CT) leaves was mixed with five mM HAuCl4 solution (1/1 ratio). The nanoparticle synthesizing reaction was permitted to progress at room conditions for various periods.

Nanomaterials dried at 100 °C for 12 hours and powdered can be stored in a sterile tube at room temperature for later use. Gold nanoparticles can be stored for a long time in a stable state without oxidation after synthesis.

With the samples taken due to color change, wavelength scans were performed with measurements in the 300-800 nm range by Perkin Elmer One UV-Vis spectrophotometry. The formation and existence of CT-AuNPs were evaluated by examining the maximum absorbance bands.

For the determination of the functional groups of phytochemicals in the CT extract responsible for the reduction reactions of AuNPs, the FTIR spectra of both the plant extract and the liquid fractions formed after the reaction were examined with (Perkin Elmer One) FTIR (spectrum range 4000-400 cm^{-1}). After the synthesis, the crystal patterns and sizes of the CT-AuNPs were defined by the Rigaku Miniflex 600 XRD (range of 20-80 2-theta, Cu∝= 1,5406) (Baran, 2020).

SEM (EVO 40 LEQ), FE-SEM, AFM (Park System XE-100), and TEM (Jeol Jem 1010) micrographs were used to determine the morphological appearance of CT-AuNPs. The elemental profile of the particles obtained after synthesis was revealed by the RadB-DMAX II computer-controlled EDX. Surface charges and size distributions of AuNPs were analyzed using zeta potentials and zeta sizer distributions (Marven) devices. The resistance of CT-AuNPs against heat treatments were examined with the data obtained with the TGA-DTA (Shimadzu TGA-50, heating rate: 10 °C/min in the range of 25-900 °C, flow rate: 20 mL/min, atmosphere: N_2(g)).

Antipathogenic Properties of CT-AuNPs

The antipathogenic effects of AuNPs were evaluated on pathogenic microorganisms by determining the Minimum Inhibition Concentration (MIC), which suppresses their growth using the Micro-Dilution method. Gram (+) *Bacillus subtilis* ATCC 11774 (*B. subtilis*) and *Staphylococcus aureus* ATCC 29213 (*S. aureus*) and gram (-) *Pseudomonas aeruginosa* ATCC27833 (*P. aeruginosa*) and *Escherichia coli* ATCC25922 (*E. coli*), and *Candida albicans* yeast were used test to antipathogenic properties of CT-AuNPs. *S. aureus*, *C. albicans*, and *E. coli* microorganisms were supplied from Inonu University Medical Faculty Hospital Microbiology Laboratory, Malatya, Turkey. *P. aeruginosa* and *B. subtilis* were also obtained from Mardin Artuklu University Microbiology Research Laboratory, Mardin, Turkey.

Microorganisms used in the assay were grown in a suitable medium (Bacteria's: Nutrient Agar, Yeast: Sabora Dextrose Agar) in an incubator at 37 °C overnight. After the growth control was done, solutions were prepared for each microorganism according to the McFarland standard 0.5 turbidity criteria (Emmanuel et al. 2015) by using microorganism colonies on the medium plates. Then, Müller Hinton medium (for bacteria) and Roswell Park Memorial Institute (RPMI) 1640 broth (for *C. albicans*) were prepared and pipetted in appropriate amounts into 96 microplate wells. Some of the microplate wells were used for sterilization and control steps for growth control. Solutions containing CT-AuNPs with different concentrations were prepared, added to the microplate wells, and the distribution of CT-AuNPs in the medium was made with a series of microdilution. The same steps were applied to antibiotics (Colistin: Gram-negative strains, Vancomycin: Gram-positive strains,

Fluconazole: C. albicans yeast), HAuCl4 solution. Microorganism solutions prepared according to Mc Farland standard 0.5 turbidity standard were transferred to microplate wells in the appropriate amount. Afterward, the microplates were incubated in an oven at 37 °C. One day after the interaction, microplates were examined for growth. The concentration of the well before the well where the growth started was determined as the MIC value where the growth was suppressed.

Cytotoxic Activities of CT-AuNPs

The cytotoxic effects of CT-AuNPs on healthy (Human Dermal Fibroblast: HDF) and cancerous (Caco-2: Colorectal adenocarcinoma; U118: Glioblastoma; Sk-ov-3: Human ovarian sarcoma) cell lines (American Type Culture Collection (ATCC) in Dicle University Scientific Research Center, Cell Culture Laboratory, Diyarbakır, Turkey) were determined by the MTT method. CaCo-2, U118, and HDF cell lines were incubated in DMEM (Dulbecco Modified Eagle) and Skov-3 cell line in RPMI (Roswell Park Memorial Institute) medium at 37 °C. The environment for growth was set to 95% air and 5% CO_2 and humidity conditions. After the cell lines were controlled by a hemocytometer and reached 80% confluence, they were re-suspended to different concentrations. Cell lines were then transferred to 96-well microplates and incubated overnight. Then, varying concentrations of AuNPs were added to the cell lines cultured in the microplate wells and left to interact with the nanoparticles for 48 hours, and then MTT solution was added to the wells and incubated for 3 hours. After waiting for another 15 minutes by adding DMSO, the data of the absorbance spectrum of the cells were measured (using Thermo Multi ScanGo) at 540 nm. By using the absorbance values of the cell lines, the concentrations of AuNPs that suppressed viability in the cell lines were calculated by the formula expressed below (Awad et al. 2019).

% viability=U/C*100

U: Absorbance values of cells treated with AgNPs; C: Absorbance values of control (healty) cells (without AgNPs in the medium).

RESULTS and DISCUSSION

Biophysical Characterization of Biogenic CT-AuNPs

UV-vis spectrum data

UV-vis spectroscopy is often used to measure molecules in solution or inorganic ions and complexes. The absorption of electromagnetic radiation by molecules or atoms varies depending on the type of atoms in the molecule. The vibrations that will occur due to the formation of NPs on the plasma surface are the result of the reduction of the charged ions in the aqueous medium. UV-vis with the samples to be taken depending on the time after the color change is observed. The presence and formation of NPs can be detected with the same maximum absorbance data to be obtained in wavelength scans made in the device. In the green synthesis of AuNPs using Dagdagan leaf extract, a color change from yellow to dark pink-red was observed 20 minutes after the extract and five mM $HAuCl_4$ solution were mixed. Depending on the intensity of color formation, samples were taken from the reaction medium, and wavelength scans were made utilizing the UV-vis spectrophotometer. Maximum absorbances were read at 553.67 nm wavelength in the measurements (Figure 2). The characteristic data (pink-red color change) indicating the formation and presence of AuNPs refers to the conversion of the Au^{+4} form to the Au^{0} form by bioreduction. The fact that the maximum absorbance value (553.67 nm) is constant for the samples measured at different time intervals as a result of the color change is proof that the reaction has taken place and is in a stable structure. The data obtained are consistent with the absorbance values of AuNPs reported in previous studies (Jafarizad et al. 2019, Babu et al. 2020, Karim et al. 2020, Rautray & Rajananthini 2020).

X-ray diffraction (XRD) analysis

By using X-ray diffraction analysis, the crystalline size, structure, and phase purity of the synthesized gold nanoparticles were confirmed. The XRD pattern of biosynthesized gold nanoparticles is depicted in Figure 3. The X-ray diffraction pattern of AuNPs produced from an aqueous extract of *Celtis tourneofortii* showed dominant peaks in the 2 range originating from the (111°), (200°), (220°), and (311°) planes with the cubic crystalline structure of nanogold at 38.00, 44.19, 64.33, and 77.26. The mean particle size was calculated as 33.35 nm using the Debye Sherer (CuK∝=1.540) equation. Based upon the consequence of XRD and peak density, it can be concluded that the CT leaf extract during the process of formation of AuNP has a respectable impact on the crystalline structure of the NPs.

FTIR analysis data

FTIR spectroscopy is a potent definition instrument for the classifying of compounds, and materials by examining them in the matchless mode of vibration and rotation. Hence, it is one of the primary techniques for classifying and definition of compounds. After biosynthesis and purifying, the MNPs can at once be reachable for functionality testing. FTIR spectrums were given in Figure 4 a,b. As seen in Figure 4 a, FTIR spectra of the plant extract and the reaction liquids obtained as a result of the synthesis were examined to determine the functional groups of phytochemicals that may be responsible for the reduction of the Au^{+4}

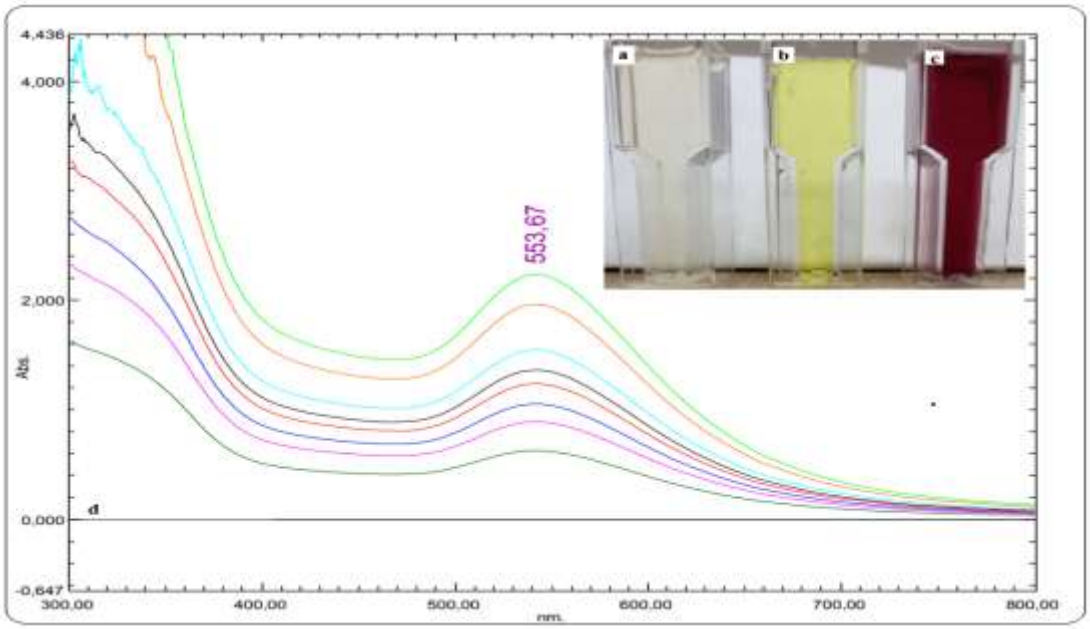

Figure 2. The formation and presence of AuNPs using CT leaf extract; a, b, and c, respectively, the 5 mM of $HAuCl_4$ solution, the plant extract, the color change resulting from the synthesis, and also d. Time-dependent UV-vis spectrum bands

Şekil 2. a. 5 mM $HAuCl_4$ çözeltisi b. *Celtis tournefortii Lam. yaprak özütü, c. Sentez sonucu AuNP'lerin oluşumuna bağlı renk değişimi görünümleri ve d. AuNP'lerin oluştuğunu ve varlığını gösteren UV-vis spektrum dataları*

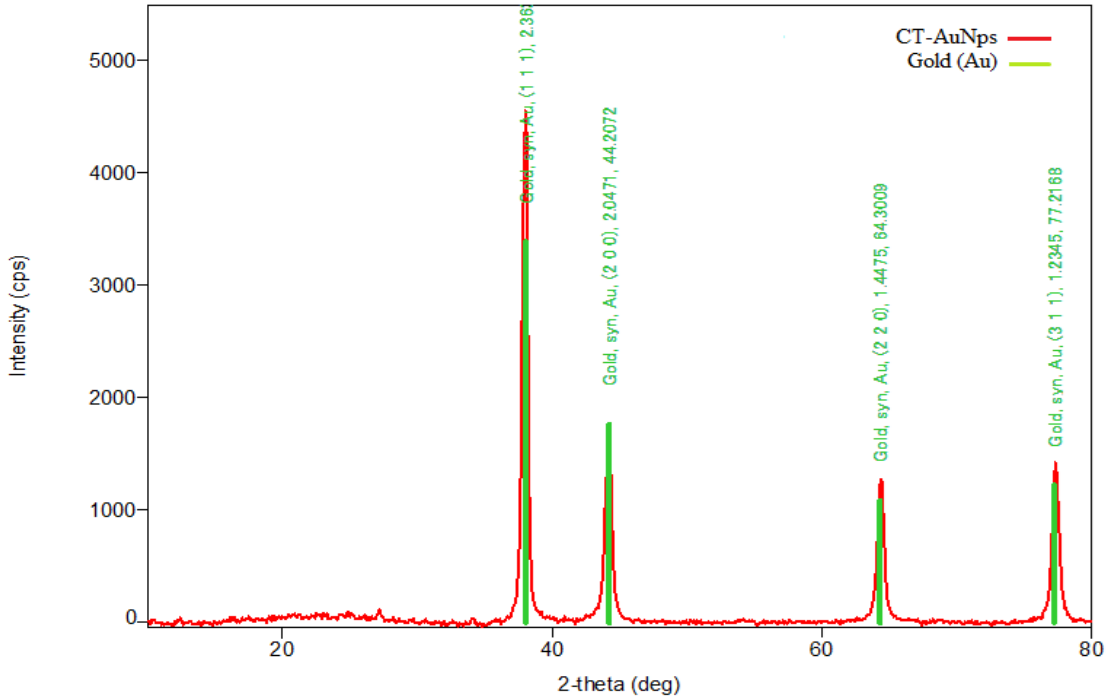

Figure 3. X-ray diffraction pattern of bio-based CT-AuNPs after synthesis

Şekil 3. Biyosentezi yapılan CT-AuNP'lerin kristal desenlerine ait X-ray kırınım deseni

form, which is responsible for bioreduction, to the Au˚ form in CT plant extract. Even though the FT-IR spectra of CT leaf aqueous extract and CT-AuNP appear to be similar, various bands of CT-AuNP are less intense than those of CT extract. CT-AuNP exhibits a slight shift in their various band positions when compared to the CT extract spectrum, indicating the essential role of CT extract in the reduction and stabilization of the formed AuNPs. In Figure 4 b, frequency shifts occur at 3288. 12 cm^{-1}, 2123. 20 cm^{-1} and 1635.27 cm^{-1} imply that alcohols/phenols (-OH; hydroxyl groups), $-CH_3$ (methylene groups), and

proteins (X-C=O; carbonyl groups) were potent in the bioreduction and stability, respectively. In alignment with numerous works, hydroxyl (-OH) and carboxylic acid (-COOH) are the two important functional groups that are related to the formation of NPs. Particularly, in the course of the genesis of NPs, the -COOH group assists in stabilization, meanwhile -OH groups help with the reduction processing (Usman et al. 2019, Padalia and Chanda 2021, Rauf et al. 2021). The carbonyl groups from the amino acid residues and peptides of proteins and the hydroxyl groups of alcohols have a great affinity to bind metals, acting as encapsulating agents to prevent the nanoparticles from aggregating (Lin et al. 2015). As a result, the FT-IR spectrum shows that the treatment of $AuHCl_4$ with the aqueous leaf extract of *C. tournefortii* resulted in the successful production of AuNPs.

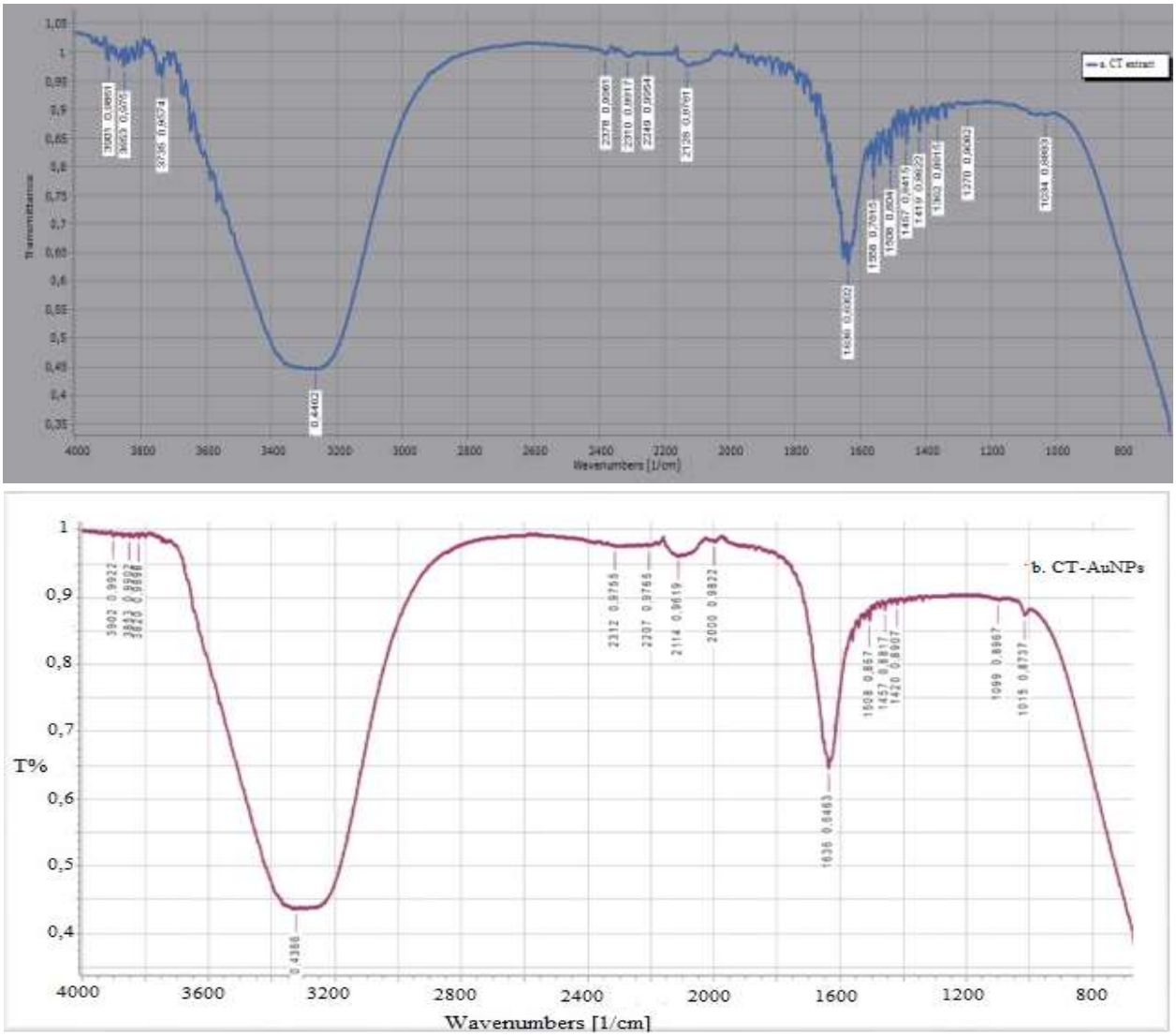

Figure 4. a- CT leaf aqueous extract FTIR spectrum b- CT-AuNPs FTIR spectrum
Şekil 4. a. CT yaprak özütü ve b. CT-AuNP'lerin FTIR spektrumları

FESEM, TEM micrographs and EDX profiles of CT-AuNPs

TEM and FESEM were used to reveal the size and morphology of the synthesized CT-AuNPs (Figure 5). The material appears to be composed of homogeneous AuNPs. The level of contamination is minimal (taking into account the biological source of the reducing agent). Biologic materials are used in the synthesis of AuNPs not only for size and shape control but also to provide superior properties to the AuNPs such as antimicrobial and cytotoxic properties. The TEM images show monodispersed and spherical nanoparticles in each case, indicating that the polyphenols act not only as a reducing agent but also as a capping agent, limiting their growth from 2 to 32 nm (Figure 5). Many of the CT-AuNPs appear to have a spherical morphology, which is often the case when no compounds are employed to favor anisotropic growth (Padalia & Chanda 2021). The dimensions of the CT-AuNPs ranged from 2 nm to 32 nm, with an average diameter of 14±6 nm.

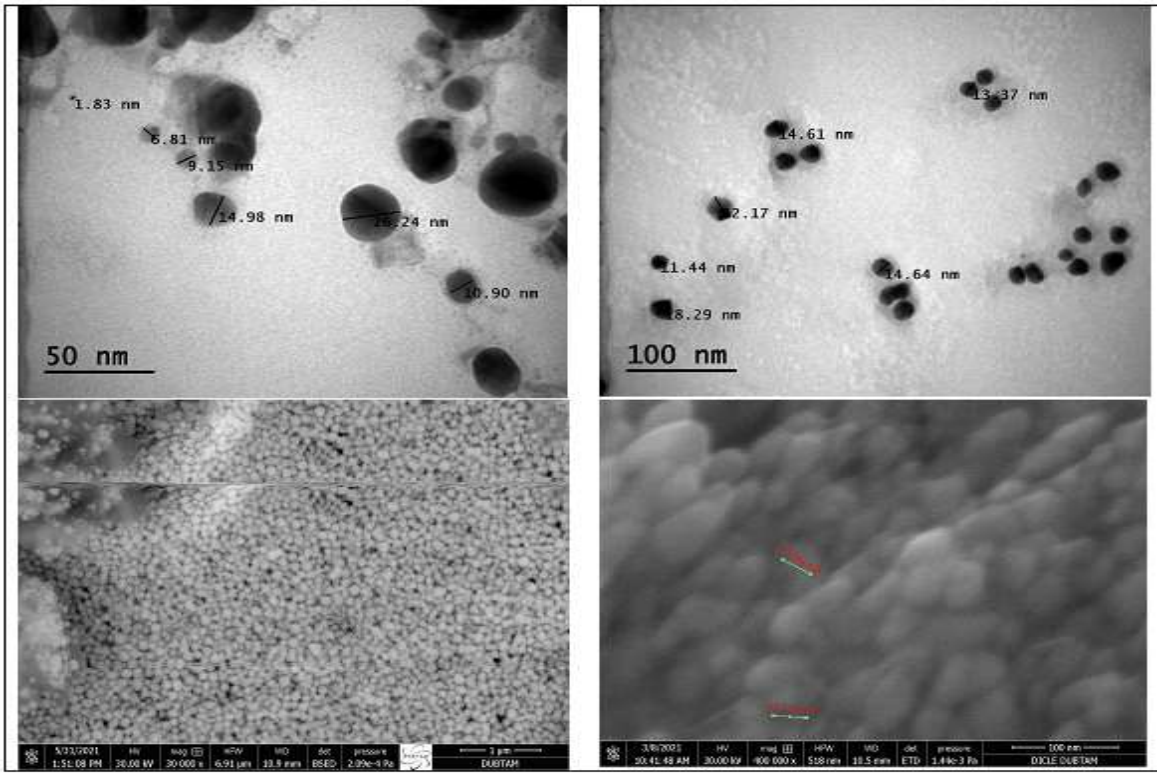

Figure 5. Morphological views of AuNPs synthesized with CT aqueous leaf extract; a and b parts indicate the TEM, c and d parts FESEM micrographs

Şekil 5. CT yaprak özütü ile sentezlenen AuNP'lerin morfolojik görünümleri; a ve b TEM, c ve d FESEM mikrografileri

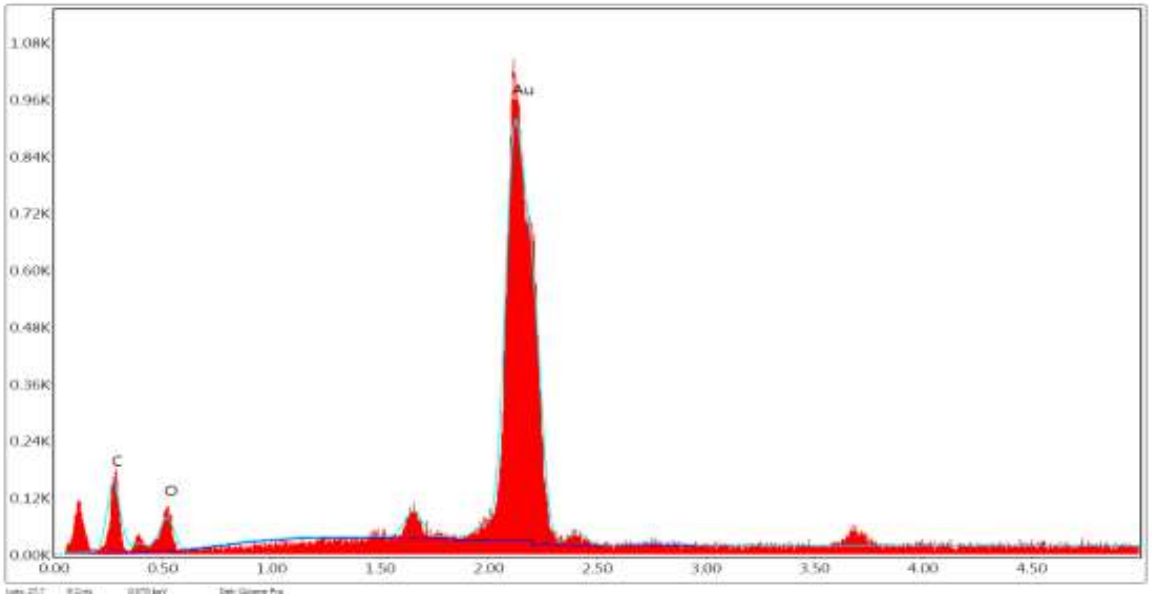

Element	Wt %	Atomic %	Error %	Net Int.	Net Error %	K Ratio	Z	R	A	F
C K	33.28	69.97	10.45	78.35	3.49	0.1460	1.2166	0.8169	0.3605	1.0000
O K	14.82	23.38	16.40	37.72	7.15	0.0231	1.1795	0.8404	0.1322	1.0000
Au L	51.90	6.65	9.23	245.80	7.12	0.4581	0.7432	1.2002	1.0554	1.1252

Figure 6. Elemental composition of particles formed as a result of biosynthesis using CT leaf aqueous extract

Şekil 6. CT yaprak özütü kullanılarak biyosentez sonrası partiküllerin element kompozisyonu

The elemental composition of CT-AuNPs was examined by EDX analysis. Absorption of metallic gold nanoparticles was determined by strong gold nanocrystal signals (51.90%) at 1.7, 2.2, 2.4, and 3.7 keV. Weak signals such as carbon (33.28%) and oxygen (14.82%) were also recorded (Figure 6). These signals are thought to originate from biomolecules on the surface of NPs and be possibly derived from CT aqueous extract as the starting material involved in stabilizing AuNPs (Doan et al. 2020, Hosny et al. 2021, Mandhata et al. 2021).

TGA-DTA analysis data of CT-AuNPs

As seen in Figure 7, the resistance of AuNPs formed as a result of synthesis to heat treatment was investigated through TGA-DTA data at 25-1000 °C. It was observed that mass losses occurred at three different temperature points. The first mass loss was between 29.25 and 248.66 °C (13.66%), the second mass loss was between 310.33 and 555.34 °C (44.58%), and the third mass loss was formed between 556.18 and 834.74 °C (15.51%) (Figure 7). The first of these mass losses was due to water loss, and the others losses occurred due to inorganic compounds. These changes demonstrated the presence of phytochemicals around the formed nanoparticles; also, these phytochemicals are responsible for the surface charge and associated with stability (Baran, et al., 2019; Doan et al., 2020; Sepahvand et al., 2020 Padalia & Chanda, 2021).

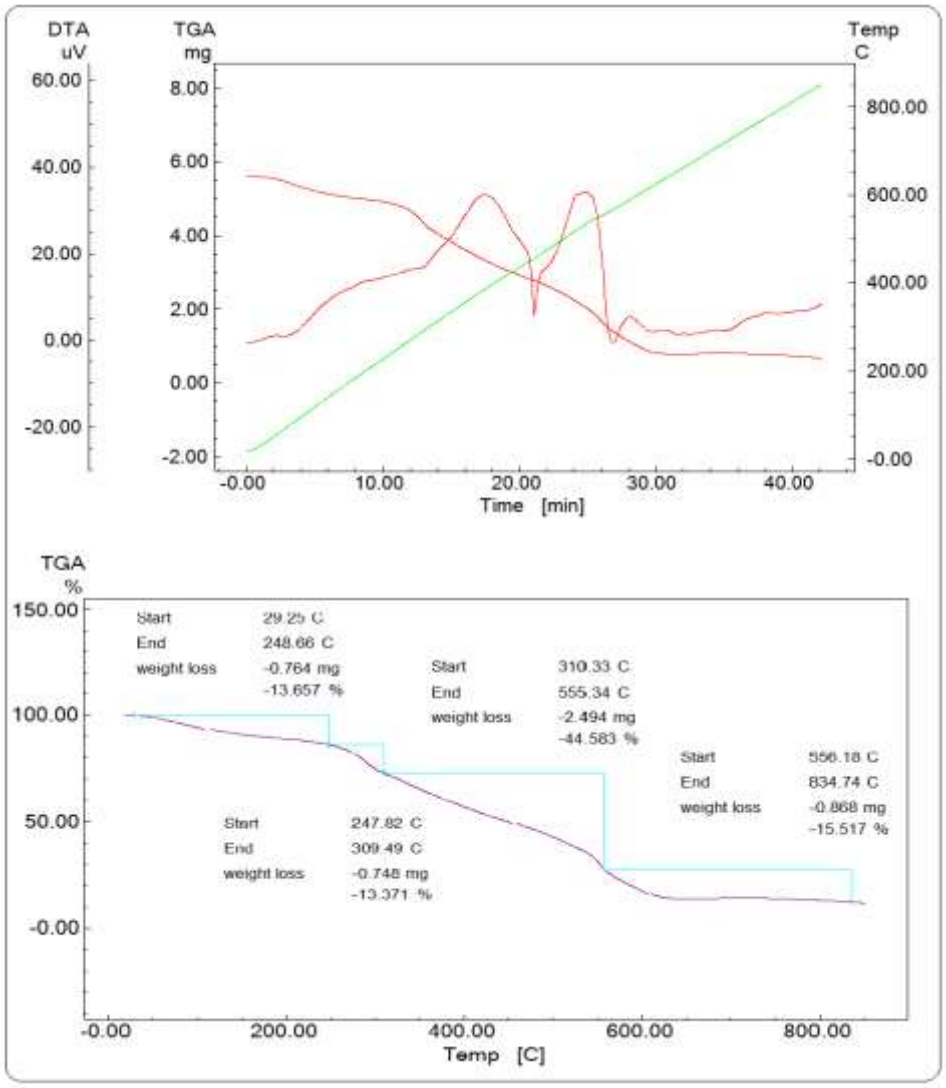

Figure 7. Temperature points at which TGA-DTA mass loss of CT-AuNPs occurs after synthesis
Şekil 7. Sentez sonrası CT-AuNP'lerin TGA-DTA sıcaklık noktalarında kütle kayıpları

Zeta potential and zeta sizer distributions data of CT-AuNPs

The stability of colloidal nanoparticles can be evaluated quantitatively using zeta potential, a measurement of the effective electrical potential on the surface of the particle. The zeta potential of the surface

charge distributions of AuNPs synthesized with CT leaf aqueous extract was determined as -16.53 mV (Figure 8a). In other environmentally friendly synthesis studies, it has been reported that the zeta potential distribution of AuNPs may have different values (Chinnaiyan et al., 2019; Khan et al., 2019; Tripathy et al., 2020).

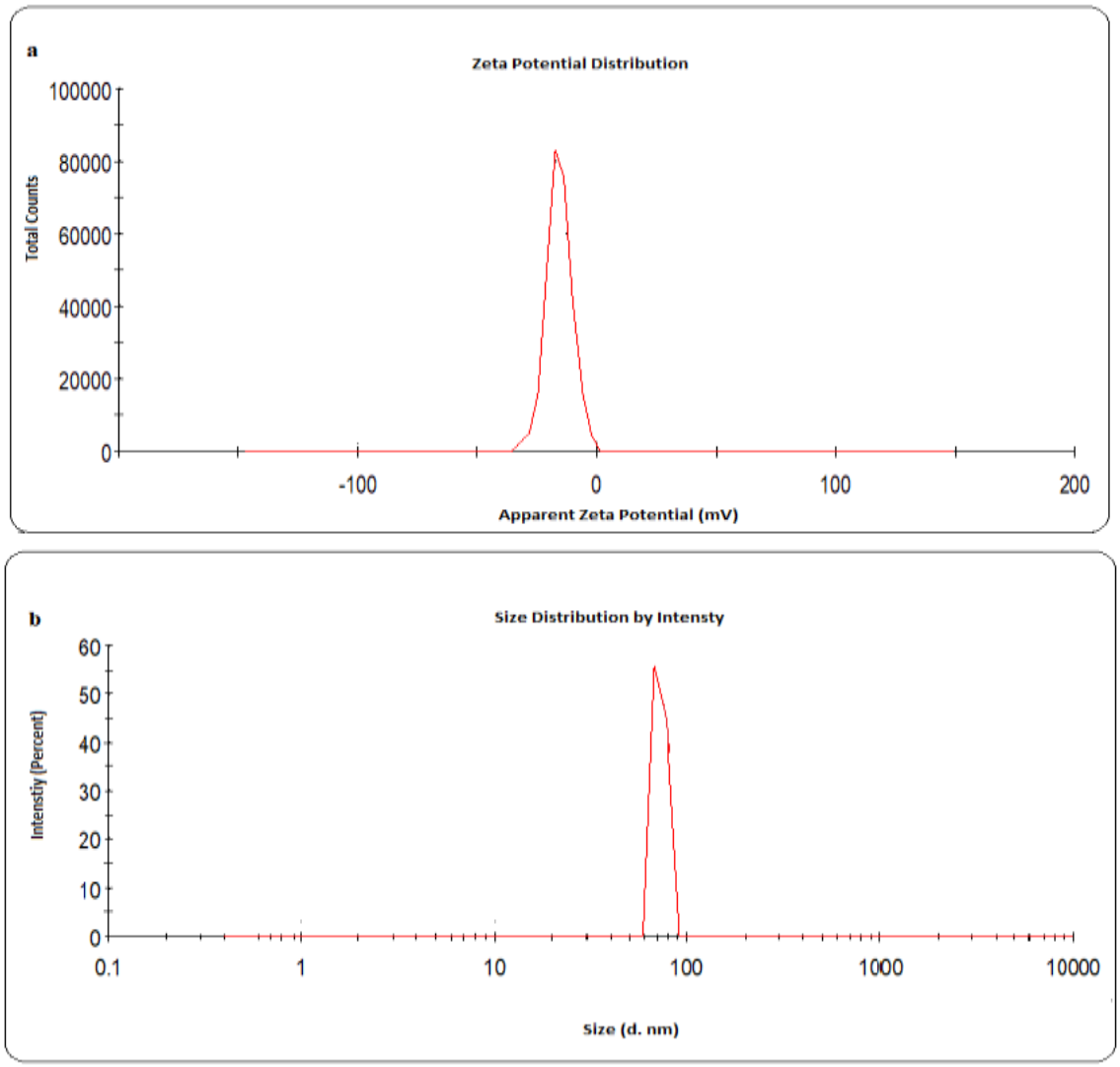

Figure 8. CT-AuNPs of after green synthesis; a. zeta potential, b. density-dependent size distribution graphs
Şekil 8. Yeşil sentez sonrasında CT-AuNP'lerin; a. zeta potansiyeli b. yoğunluğa bağlı boyut dağılımı grafileri

It is very important that AuNPs, as therapeutic agents, especially in drug delivery systems, ensure their stability under challenging conditions such as cell or blood circulation (Giljohann et al. 2010). The negative zeta potential distributions of the synthesized AuNPs provide pH stability, but also prevent the formation of properties that destabilize such as aggregation and fluctuation. Phytochemicals are the factor that causes the surface charge distribution of AuNPs to be negative (Khan et al. 2019, Webster 2020).

It has been reported that gold nanoparticles show different size distributions in environmentally friendly synthesis studies using plant materials (Usman et al., 2019; Perveen et al., 2021).

AFM micrograph of CT-AuNPs

AFM analysis gives us a grip on the topography, and roughness of metallic nanoparticles. The color scale helps determine the average size range on the scale bar. AFM imaging was applied in distinct magnification ranges of 12 and 50 µm (Figure 9). The AFM analysis performed to examine the topographic distribution of the synthesized CT-AuNPs and to evaluate their morphological structure and dimensions revealed that they were monodisperse, spherical in morphology, and less than 50 nm in size, which was consistent with other studies (Francis et al. 2017, Rauf et al. 2021).

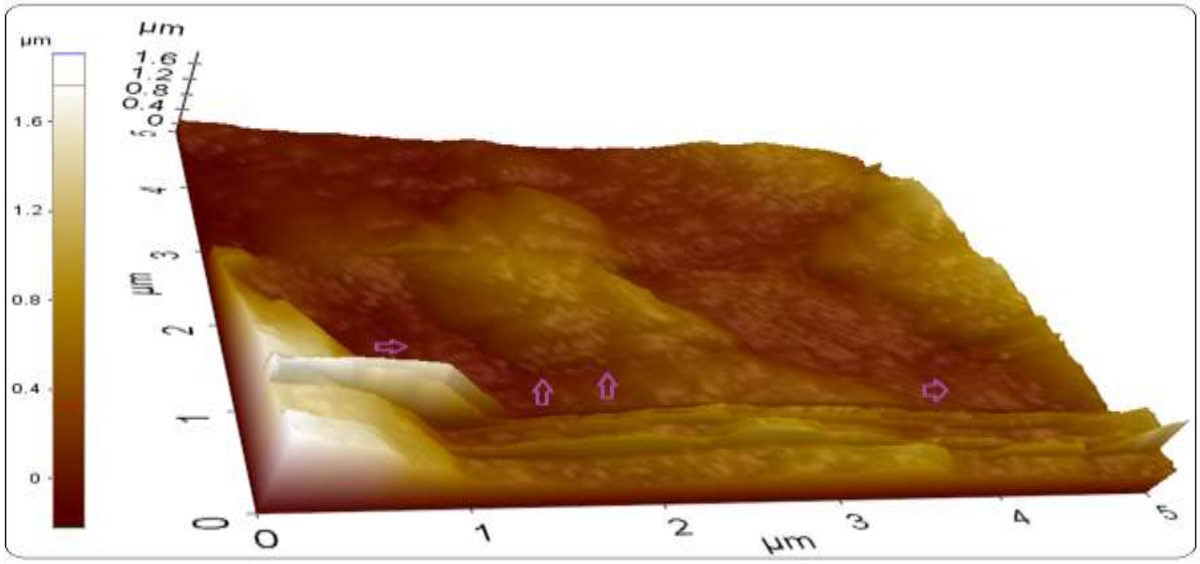

Figure 8. Topographic image of AuNPs synthesized with CT-aqua leaf extract
Şekil 8. CT-sulu yaprak özütüyle sentezlenen AuNP'lerin topografik görüntüsü

Biomedical Applications of CT-AuNPs

Antimicrobial effects of synthesized AuNPs

Regular and insufficient use of antibiotics has improved drug resistance to pathogen bacterial strains owing to genetic mutations. This situation makes the present antibiotics lesser potent for treating chronic illnesses. The improvement of strong and cost-potent drugs is the preference of recent studies. Metallic nanoparticles have superior properties that can easily serve these purposes. AuNPs interact with microorganisms due to electrostatic attraction (Babu et al. 2020). AuNPs induce an increase in Reactive Oxygen Species (ROS) and inhibit important steps of energy metabolism and transcription. After the interaction with nanoparticles, microorganisms reduce the ATP level by changing the membrane potential and inhibiting the ATPase activity, thus slowing down the metabolism. AuNPs also accelerate the biological collapse of the microorganism by suppressing the binding of tRNA to the small subunit of the ribosome (Cui et al. 2012, Jha et al. 2017, Babu et al. 2020, Donga et al. 2020, Webster 2020). The microdilution method was used to determine the MIC value of CT-AuNPs, HAuCL4 solution, and standard antibiotics on pathogen strains. At concentrations ranging from 0.01 to 0.50 g/mL, the synthesized CT-AuNPs were found to have a strong inhibitory effect on the growth of the tested organisms (Table 1).CT-AuNPs exhibited more effectiveness on gram-positive and negative strains at very low concentrations when compared to tested standard antibiotics (Colistin and Vancomycin), and HAuCI4 solution. Moreover, it was observed that the suppressive effect of CT-AuNPs on the C. albicans yeast was four times lower than the standard antibiotic (Fluconazole) and eight times lower concentration than the HAuCI4 solution when compared (Table 1). Researchers reported similar results that support in this results (Baran et al., 2020; Baran et al., 2021).

Table 1. Minimum Inhibition Concentrations (µg mL^{-1}) value of CT-AuNPs, standard antibiotics and Gold (III) chloride solution ($HAuCl_4$)
Çizelge 1.

Pathogen Microorganisms	CT-AuNPs	$HAuCl_4$	Standard Antibiotics*
S. aureus	0.02	1.00	2.00
B. subtilis	0.01	0.50	0.50
E. coli	0.03	2.00	4.00
P. aeruginosa	0.50	1.00	4.00
C. albicans	0.25	2.00	1.00

* Colistin for gram negatives, Vancomycin for gram positives, Fluconazole for yeast.

Cytotoxic effects of CT-AuNPs

Various properties of nanomaterials play a decisive role in their toxic effect. These include the shape of the NPs, but also their properties such as concentration, charge, exposure time, the chemistry of the surface composition, degree of deposition, and size. When the cell size is small, AuNPs easily pass through the cell

membrane and cause changes in the morphological structure of the cell. They cause an increase in ROS and changes in the nuclear structure. They induce apoptosis by activating caspase enzymes, besides, they spread the apoptotic signal by increasing cytochrome c release by affecting mitochondrial permeability, and as a result, they cause cell death (Rolim et al. 2019, Barabadi et al. 2020, Donga et al. 2020, Webster 2020). Various properties of nanoparticles are the characteristics that determine their effectiveness in toxic activity. Among these features of AuNPs; are surface charges, concentrations, interaction times, shapes, degrees of deposition, and sizes are the most important (Remya et al. 2015, Swamy et al. 2015). The cell viability and suppressing concentrations of AuNPs synthesized by CT leaf extract on CaCo-2, Skov-3, and U118 cell lines were investigated using the MTT method (Table 2). 100 µg/mL concentration of CT-AuNPs showed a suppressive effect on viability in all cell lines. Also, the 25 and 200 µg/mL concentrations of CT-AuNPs in healthy cell lines (HDF) caused suppression of proliferation by 74.66% and 50.6%. Moreover, the 25 µg/mL CT-AuNPs concentration exhibited suppressing activity on the proliferation of the CaCo-2 cell line at 88.58% percentage. On the other hand, the 100 µg/mL CT-AuNPs concentration suppressed growing of the U118 and Skov-3 cell lines at 92.50% and 92.46% percent respectively.

Table 2. Cytotoxic effects of CT-AuNPs on cell lines
Çizelge 2.

	Concentrations (µg/mL)			
Cell Lines	**25**	**50**	**100**	**200**
HDF	25.34*	27.55	33.80	49.43
CaCo-2	11.42	11.42	11.45	11.41
U118	68.54	58.89	7.54	10.78
Skov-3	58.79	51.86	7.50	9.49

*% viability rates of cells lines

CONCLUSION

This study demonstrated that AuNPs can be produced without the use of chemicals from Celtis tournefortii leaf extract in an environmentally friendly, toxic residue-free, and cost-effective method. UV-vis spectroscopy, UV-vis, XRD, FTIR, TEM, AFM, FESEM, EDX, TGA-DTA, zeta potential, and zeta sizer techniques were used to characterize CT-AuNPs. Gold nanoparticles prepared with this plant have a strong antipathogenic and cytotoxic effect, with a homogeneous distribution and a spherical appearance with a mean size of 31.30 nm, and the absence of any significant toxicity was evaluated and verified pending the current work. CT-AuNP showed good anticancer properties against CaCo-2, U118, and Skov-3. Hence, Celtis tournefortii leaf aqueous extract stabilized AuNPs be able to effectually as a vigorous means against cancerous cell lines. CT-AuNP exhibited significant antimicrobial activity against varied human pathogenic bacteria and yeast. As a whole, the study's findings highlighted green AuNPs' promising potential for anticancer and antimicrobial activity. As a result, a translation of the methodology is proposed as a simple, commercially viable, and environmentally friendly therapeutic approach in the field of nanomedicine and biomedicine.

ACKNOWLEDGEMENT

This study was created by using some of the doctoral thesis data of Ayşe BARAN. The authors thank Dr. Sevgi İrtegün KANDEMİR from Dicle University for his valuable contribution and comments on the manuscript

Author's Contributions

The authors declare that they have contributed equally to the article.

Statement of Conflict of Interest

Authors have declared no conflict of interest.

REFERENCES

Abu-Dief AM, Abdel-Rahman LH, Abd-El Sayed MA, Zikry MM, Nafady A 2020. Green Synthesis of AgNPs Utilizing *Delonix regia* Extract as Anticancer and Antimicrobial Agents. *ChemistrySelect 5*(42), 13263–13268.

Al-ogaidi I, Salman MI, Mohammad FI, Aguilar Z, Al-M, Hadi YA, Al-rhman RMA 2017. Antibacterial and Cytotoxicity of Silver Nanoparticles Synthesized in Green and Black Tea. *World J. Exp. Biosci. 5*(1), 39–45.

Arroyo G V., Madrid AT, Gavilanes AF, Naranjo B, Debut A, Arias MT, Angulo Y 2020. Green Synthesis of Silver Nanoparticles for Application In Cosmetics. *J. Environ. Sci. Heal. - Part A Toxic/Hazardous Subst. Environ. Eng. 55*(11), 1304–1320.

Asghar MA, Zahir E, Shahid SM, Khan MN, Asghar MA, Iqbal J, Walker G 2018. Iron, Copper and Silver Nanoparticles, Green Synthesis Using Green And Black Tea Leaves Extracts And Evaluation of Antibacterial, Antifungal and Aflatoxin B1 adsorption Activity. *LWT - Food Sci. Technol. 90*, 98–107.

Awad M, Eisa N, Virk P, Hendi A, Ortashi K, Mahgoub AA, Elobeid, Mai, Eissa F 2019. Green Synthesis of

Gold Nanoparticles: Preparation, Characterization, Cytotoxicity, And Anti-Bacterial Activities. *Mater. Lett. 256*, 126608.

Babu B, Palanisamy S, Vinosha M, Anjali R, Kumar P, Pandi B, Tabarsa M, You SG, Prabhu NM 2020. Bioengineered Gold Nanoparticles From Marine Seaweed Acanthophora Spicifera for Pharmaceutical Uses: Antioxidant, Antibacterial and Anticancer Activities. *Bioprocess Biosyst. Eng. 43*(12), 2231–2242.

Barabadi H, Webster T, Vahidi H, Sabori H, Damavandi Kamali K, Jazayeri Shoushtari F, Mahjoub MA, Rashedi M, Mostafavi E, Medina Cruz D, Hosseinic O, Saravanah M 2020. Green Nanotechnology-Based Gold Nanomaterials for Hepatic Cancer Therapeutics: A Systematic Review. *Iran. J. Pharm. Res. 19*(3), 3–17.

Baran A, Keskin C, Kandemir SI 2022. Rapid Biosynthesis of Silver Nanoparticles by *Celtis tournefortii* LAM. Leaf Extract; Investigation of Antimicrobial and Anticancer Activities. *KSU J. Agric Nat 25*(4), 72-84.

Baran, M. F., Saydut A 2019. Gold Nanomaterial Synthesis and Characterization. Dicle Univ. J. Eng. 10(3), 1033–1040.

Baran, M.F., Acay, H., Keskin C 2020. Determination of Antimicrobial and Toxic Metal Removal Activities of Plant-Based Synthesized (*Capsicum annuum* L. Leaves), Ecofriendly, Gold Nanomaterials. *Glob. Challenges 2020*, 1–7.

Baran, M.F., Acay, H., Keskin, C., Aygün, H., Yildirim A 2019. Synthesis and Determination of Antimicrobial Properties of TiO_2NPs Using Nigella sativa L. Extract. *EJONS Math. Eng. Nat. Med. Sci. 7*, 69–75.

Baran, MF., Keskin, C., Atalar, MN., Baran A 2021. Environmentally Friendly Rapid Synthesis of Gold Nanoparticles from *Artemisia absinthium* Plant Extract and Application of Antimicrobial Activities. *J. Inst. Sci. Technol. 11*(1), 365–375.

Baran MF 2019a. Synthesis Of Silver Nanoparticles (AgNP) With *Prunus avium* Cherry Leaf Extract and Investigation of its Antimicrobial Effect. *Dicle Univ. J. Eng. 10*(1), 221–227.

Baran MF 2019b. Evaluation of Green Synthesis and Anti-Microbial Activities of AgNPs Using Leaf Extract of Hawthorn Plant. *Res. Eval. Sci. Math. 2019*(3), 110–120.

Baran MF 2019c. Synthesis, Characterizatıon, and Investigation of Antimicrobial Activity of Silver Nanoparticles from *Cydonia oblonga* Leaf. *Appl. Ecol. Environ. Res. 17*(2), 2583–2592.

Chinnaiyan SK, Soloman AM, Perumal RK, Gopinath A, Balaraman M 2019. 5 Fluorouracil-Loaded Biosynthesised Gold Nanoparticles for the *In Vitro* Treatment of Human Pancreatic Cancer Cell. *IET Nanobiotechnol. 13*(8), 824–828.

Cui Y, Zhao Y, Tian Y, Zhang W, Lü X, Jiang X 2012. The Molecular Mechanism Of Action Of Bactericidal Gold Nanoparticles on *Escherichia coli*. *Biomater. 33*(7), 2327–2333.

Doan VD, Thieu AT, Nguyen TD, Nguyen VC, Cao XT, Nguyen TLH, Le VT 2020. Biosynthesis of Gold Nanoparticles Using *Litsea cubeba* Fruit Extract for Catalytic Reduction of 4-Nitrophenol. *J. Nanomater. 2020*, 1–10.

Donga S, Bhadu GR, Chanda S 2020. Antimicrobial, Antioxidant, and Anticancer Activities of Gold Nanoparticles Green Synthesized Using *Mangifera indica* Seed Aqueous Extract. *Artif. Cells Nanomed. Biotechnol. 48*(1), 1315–1325.

Emmanuel R, Palanisamy S, Chen S, Chelladurai K, Padmavathy S, Saravanan M, Prakash P, Ali MA, Al-hemaid, Fahad MA 2015. Antimicrobial Efficacy of Green Synthesized Drug Blended Silver Nanoparticles Against Dental Caries And Periodontal Disease Causing Microorganisms. *Mater. Sci. Eng. C. 56*, 374–379.

Francis S, Joseph S, Koshy EP, Mathew B 2017. Green Synthesis And Characterization of Gold and Silver Nanoparticles Using *Mussaenda glabrata* Leaf Extract and Their Environmental Applications To Dye Degradation. *Environ. Sci. Pollut. Res. 24*, 17347–17357.

Gecibesler IH 2019. Antioxidant Activity and Phenolic Profile of Turkish *Celtis tournefortii*. *Chem. Nat. Compd. 55*(4), 738–742.

Giljohann DA, Seferos DS, Daniel WL, Massich MD, Patel PC, Mirkin CA 2010. Gold Nanoparticles for Biology and Medicine. *Angew. Chemie - Int. Ed. 49*(19), 3280–3294.

González-Ballesteros N, Prado-López S, Rodríguez-González JB, Lastra M, Rodríguez-Argüelles MC 2017. Green Synthesis of Gold Nanoparticles Using Brown Algae *Cystoseira baccata*: Its Activity In Colon Cancer Cells. *Colloids Surf. B. 153*, 190–198.

Haddada M Ben, Koshel D, Yang Z, Fu W, Spadavecchia J, Pesnel S, Morel AL 2019. Proof of Concept of Plasmonic Thermal Destruction Of Surface Cancers By Gold Nanoparticles Obtained By Green Chemistry. *Colloids Surf. B. 184*, 110496.

Hatipoğlu A 2021. Green Synthesis of Gold Nanoparticles from *Prunus cerasifera, Pissardii nigra* Leaf and Their Antimicrobial Activities On Some Food Pathogens. *Prog. Nutr. 23*(3), e2021241.

Hosny M, Fawzy M, El-Borady OM, Mahmoud AED 2021. Comparative Study Between Phragmites Australis Root And Rhizome Extracts For Mediating Gold Nanoparticles Synthesis and Their Medical and Environmental Applications. *Adv. Powder Technol. 32*(7), 2268–2279.

Jafarizad A, Safaee K, Vahid B, Khataee A, Ekinci D 2019. Synthesis And Characterization Of Gold Nanoparticles Using *Hypericum perforatum* and Nettle Aqueous Extracts: A Comparison With Turkevich Method. *Environ. Prog. Sustain. Energy*

38(2), 508–517.

Jha P, Saraf A, Rath D, Sharma D 2017. Green Synthesis and Antimicrobial Property of Gold Nanoparticles : a Review. *World J. Pharm. Medical Res. 3*(8), 431–435.

Karim MR, Han TH, Sawant SY, Shim J jin, Lee MY, Kim WK, Kim JS, Cho MH 2020. Microbial Fuel Cell-Assisted Biogenic Synthesis of Gold Nanoparticles and its Application to Energy Production and Hydrogen Peroxide Detection. *Korean J. Chem. Eng. 37*(7), 1241–1250.

Keser S, Keser F, Kaygili O, Tekin S, Turkoglu I, Demir E, Turkoglu S, Karatepe M, Sandal S, Kirbag S 2017. Phytochemical Compounds and Biological Activities of *Celtis tournefortii* Fruits . *Anal. Chem. Lett. 7*(3), 344–355.

Khan AU, Khan M, Malik N, Cho MH, Khan MM 2019. Recent Progress Of Algae And Blue–Green Algae-Assisted Synthesis of Gold Nanoparticles for Various Applications. *Bioprocess Biosyst. Eng. 42*(1), 1–15.

Kumar V, Singh DK, Mohan S, Gundampati RK, Hasan SH 2017. Photoinduced Green Synthesis of Silver Nanoparticles Using Aqueous Extract Of *Physalis angulata* and its Antibacterial and Antioxidant Activity. *J. Environ. Chem. Eng. 5*(1), 744–756.

Kumar V, Singh S, Srivastava B, Bhadouria R 2019. Journal of Environmental Chemical Engineering Green Synthesis of Silver Nanoparticles Using Leaf Extract of *Holoptelea integrifolia* and Preliminary Investigation of its Antioxidant, Anti-inflammatory, Antidiabetic and Antibacterial Activities. *J. Environ. Chem. Eng. 7*(3), 103094.

Lin Z, Wu J, Xue R, Yang Y (2005). Spectroscopic characterization of Au3+ biosorption by waste biomass of *Saccharomyces cerevisiae*. *Spectrochim. Acta - A: Mol. Biomol. 61*(4), 761-765.

Mandhata CP, Sahoo CR, Mahanta CS, Padhy RN 2021. Isolation, Biosynthesis and Antimicrobial Activity of Gold Nanoparticles Produced with Extracts Of *Anabaena spiroides*. *Bioprocess Biosyst. Eng. 44*(8), 1617–1626.

Marslin G, Selvakesavan RK, Franklin G, Sarmento B, Dias ACP 2015. Antimicrobial Activity of Cream Incorporated with Silver Nanoparticles Biosynthesized from *Withania somnifera*. *Int. J. Nanomedicine 10*, 5955–5963.

Mehravani B, Ribeiro AI, Zille A 2021. Gold Nanoparticles Synthesis and Antimicrobial Effect on Fibrous Materials. *Nanomater. 11*(5), 1–37.

Mohammadi F, Yousefi M, Ghahremanzadeh R 2019. Green Synthesis, Characterization and Antimicrobial Activity of Silver Nanoparticles (AgNPs) Using Leaves and Stems Extract of Some Plants. *Adv. J. Chem. A 2*(4), 266–275.

Padalia H, Chanda S 2021. Antioxidant and Anticancer Activities of Gold Nanoparticles Synthesized Using Aqueous Leaf Extract of *Ziziphus nummularia*. *Bionanosci. 11*(2), 281–294.

Pandiyan N, Murugesan B, Arumugam M, Sonamuthu J, Samayanan S, Mahalingam S 2019. Ionic Liquid-A Greener Templating Agent with *Justicia adhatoda* Plant Extract Assisted Green Synthesis Of Morphologically Improved Ag-Au/Zno Nanostructure and it's Antibacterial and Anticancer Activities. *J. Photochem. Photobiol. B Biol. 198*, 111559.

Patil MP, Singh RD, Koli PB, Patil KT, Jagdale BS, Tipare AR, Kim G 2018. Antibacterial Potential of Silver Nanoparticles Synthesized Using *Madhuca longifolia* Flower Extract As A Green Resource. *Microb. Pathog. 121*, 184–189.

Patra S, Mukherjee S, Kumar A, Ganguly A, Sreedhar B, Ranjan C 2015. Green Synthesis, Characterization Of Gold and Silver Nanoparticles and Their Potential Application for Cancer Therapeutics. *Mater. Sci. Eng. C 53*, 298–309.

Perveen K, Husain FM, Qais FA, Khan A, Razak S, Afsar T, Alam P, Almajwal AM, Abulmeaty MMA 2021. Microwave-Assisted Rapid Green Synthesis of Gold Nanoparticles Using Seed Extract of *Trachyspermum ammi*: Ros Mediated Biofilm Inhibition and Anticancer Activity. *Biomolecules 11*(2), 1–16.

Rauf A, Ahmad T, Khan A, Maryam, Uddin G, Ahmad B, Mabkhot YN, Bawazeer S, Riaz N, Malikovna BK, Almarhoon ZM, Al-Harrasi A 2021. Green Synthesis and Biomedicinal Applications of Silver And Gold Nanoparticles Functionalized with Methanolic Extract of *Mentha longifolia*. *Artif. Cells, Nanomedicine Biotechnol. 49*(1), 194–203.

Rautray S, Rajananthini AU 2020. Therapeutic Potential of Green, Synthesized Gold Nanoparticles. *BioPharm Int. 33*(1), 30–38.

Remya RR, Rajasree SRR, Aranganathan L, Suman TY 2015. An Investigation on Cytotoxic Effect of Bioactive Agnps Synthesized Using Cassia *Fistula* Flower Extract On Breast Cancer Cell MCF-7. *Biotechnol. Reports 8*, 110–115.

Rolim WR, Pelegrino MT, de Araújo Lima B, Ferraz LS, Costa FN, Bernardes JS, Rodigues T, Brocchi M, Seabra AB seabra 2019. Green Tea Extract Mediated Biogenic Synthesis of Silver Nanoparticles: Characterization, Cytotoxicity Evaluation, and Antibacterial Activity. *Appl. Surf. Sci. 463*, 66–74.

Satpathy S, Patra A, Ahirwar B, Hussain MD 2020. Process Optimization for Green Synthesis of Gold Nanoparticles Mediated by Extract of *Hygrophila spinosa* T. Anders and Their Biological Applications. *Phys. E Low-Dimensional Syst. Nanostructures 121*, 113830.

Sepahvand M, Buazar F, Sayahi MH 2020. Novel Marine-Based Gold Nanocatalyst In Solvent-Free Synthesis of Polyhydroquinoline Derivatives: Green

and Sustainable Protocol. *Appl. Organomet. Chem. 34*(12), 1–11.

Shankar PD, Shobana S, Karuppusamy I, Pugazhendhi A, Ramkumar VS, Arvindnarayan S, Kumar G 2016. A Review on The Biosynthesis of Metallic Nanoparticles (Gold and Silver) Using Bio-Components of Microalgae: Formation Mechanism and Applications. *Enzyme Microb. Technol. 95*, 28–44.

Some S, Bulut O, Biswas K, Kumar A, Roy A, Sen IK, Mandal A, Franco OL, İnce İA, Neog K, Das S, Pradhan S, Dutta S, Bhattacharjya D, Saha S, Mohapatra PD, Bhuimali A, Kati A, Mandal AK, Yilmaz MD, Ocsoy I 2019. Effect of Feed Supplementation with Biosynthesized Silver Nanoparticles Using Leaf Extract of *Morus Indica* L. V1 on *Bombyx mori* L. (Lepidoptera: Bombycidae). *Sci. Rep. 9*(1), 1–13.

Swamy MK, Akhtar MS, Mohanty SK, Sinniah UR 2015. Synthesis And Characterization Of Silver Nanoparticles Using Fruit Extract of *Momordica cymbalaria* and Assessment of Their *In vitro* Antimicrobial, Antioxidant and Cytotoxicity Activities. *Spectrochim. Acta - Part A Mol. Biomol. Spectrosc. 151*, 939–944.

Tripathy A, Behera M, Rout AS, Biswal SK, Phule AD 2020. Optical, Structural, and Antimicrobial Study Of Gold Nanoparticles Synthesized Using an Aqueous Extract of *Mimusops elengi* Raw Fruits. *Biointerface Res. Appl. Chem. 10*(6), 7085–7096.

Usman AI, Aziz AA, Noqta OA 2019. Green Sonochemical Synthesis of Gold Nanoparticles Using Palm Oil Leaves Extracts. *Mater. Today Proc. 7*, 803–807.

Uzma M, Prasad D, Sunayana N, Vinay R, Shilpashree H. 2022. Studies of *in vitro* Antioxidant And Anti-Inflammatory Activities Of Gold Nanoparticles Biosynthesised from a Medicinal Plant, *Commiphora wightii*. *Mater. Technol.* 37(9), 915–925.

Velmurugan P, Anbalagan K, Manosathyadevan M, Lee KJ, Cho, MinJung-Hee Park, Sae-Gang Oh K-SB, Oh B-T, Lee SM 2014. Green Synthesis of Silver and Gold Nanoparticles Using *Zingiber officinale* Root Extract and Antibacterial Activity of Silver Nanoparticles Against Food Pathogens. *Bioprocess Biosyst. Eng. 37*(10), 1935–1943.

Webster TJ 2020. Recent Developments in the Facile Bio-Synthesis of Gold Nanoparticles (AuNPs) and Their Biomedical Applications. *Int. J. Nanomedicine. 15*, 275–300.

Yıldırım I, Uğur Y, Kutlu T 2017. Investigation of Antioxidant Activity and Phytochemical Compositions of *Celtis tournefortii*. *Free Radic. Antioxid. 7*(2), 160-165.